A Microwave/Millimeter Wave Dual-Band Shared Aperture Patch Antenna Array

ZONGXIN WANG AND ZEQIN HUANG

School of Information Science and Engineering, Southeast University, Nanjing 210096, China

Corresponding author: Zongxin Wang (wangzx@seu.edu.cn)

ABSTRACT This paper describes the design of microwave/millimeter wave dual-band patch antenna array with shared aperture. The antenna array is designed of stack structure of three printed circuit boards. The Ka-band patches are fed directly with microstrip lines of the Ka-band power divider network and the E-band patches are coupling fed by the E-band power divider network through slots cut in the antenna ground. An antenna unit is studied, fabricated and measured firstly to verify the feasibility of the shared aperture structure. Finally, a shared aperture antenna array consists of a 2 × 4 Ka-band array and an 8 × 16 E-band array is designed based on the antenna unit. The E-band and the Ka-band feeding network are carefully designed to reduce the reflections, and the Ka-band feeding network combines series feed and parallel feed in order to save space. The shared aperture antenna array is fabricated and measured, and the results are presented. In order to measure the E-band array, the main port of the E-band power divider is connected to a standard WR12 waveguide through an antipodal fin-line waveguide to microstrip transition.

INDEX TERMS Dual frequency band, shared aperture, microstrip antenna array.

I. INTRODUCTION

With the rapid development of communication technology, antennas operating at different frequencies are required. In a radar system, the use of a dual-frequency band can effectively improve the radar performance, as the electromagnetic wave in the low-frequency band has strong penetration ability, less attenuation and a low false alarm rate, while the electromagnetic wave in the high-frequency band has high resolution and a strong target recognition ability. However, each band requires an exclusive antenna; thus, a multiband system needs more than one antenna, and the weight, size and cost are usually restricted. The constraints can be balanced by adopting antennas capable of working at different bands while sharing the same aperture. Many dual-frequency-band antennas sharing the same aperture were reported around 1995 [1]–[4], and the shared aperture antenna concept was put forward by Axness *et al.* [2]. Most of the shared aperture antennas are based on printed circuit board (PCB) technology, which is cost effective, while waveguide antennas are bulky and difficult to manufacture and are especially difficult to use in a phased array feed. C/L-, C/X- or S/X-band shared-aperture microstrip patch antennas are often reported to be dual-band or multiband antennas [5]–[10], as it is relatively easier to

arrange patches of higher and lower frequency due to the even ratio between higher and lower operating frequencies and because it is relatively easier to arrange the feed lines due to their lower operating frequencies. In addition to the dual-band antenna with two patch combination types, there is another dual-band antenna that uses both patches and slots as radiators [11], where each patch radiator works in the low-frequency band and the slots etched on each patch are used as high-frequency radiators.

In this paper, a shared-aperture microwave/millimeter wave dual-band microstrip patch antenna array is studied. The antenna array is required to operate at 84GHz (E-band) and 28GHz (Ka-band). The frequency ratio between the higher and lower frequency is nearly 3:1, so the patches and the feed structures must be carefully designed. The shared-aperture E/Ka dual band antenna unit is studied at first, then the array is formed based on the antenna unit. Parallel-fed is hard to be applied solely to feed the array for the narrow space, so the series-fed is employed in the internal of the array, and parallel-fed is employed outside the array respectively as that in [12], [13].

II. DESIGN OF THE E/KA DUAL BAND SHARED APERTURE ANTENNA UNIT

A stacked configuration is used to design the shared aperture antenna unit (SAAU), see Figure 1. The whole structure is
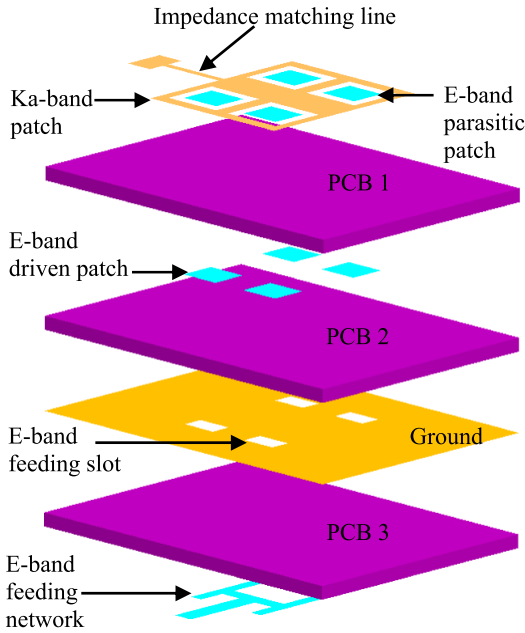
FIGURE 1. Laminated structure of the E-/Ka-band shared aperture patch antenna.

composed of three Rogers 5880 PCBs which are laminated together tightly. Four E-band parasitic patches and a Ka-band patch are printed on the top of the PCB 1, the Ka-band patch has four square perforations where the E-band parasitic patches are set; four E-band driven patches are printed at the back side of PCB1, and the stackedstructure of E-band parasitic and driven patches is used to broaden the band width of the antenna [14]; the ground plane and the E-band feed network are printed on the top and back of PCB 3 respectively; the E-band patches are fed by the microstrip line network coupling through slots on the ground plane at the top of PCB 3; PCB2 is a bare board whose primary role is to support PCB1.

There are two details to consider in the design. Firstly, since the E-band parasitic patches are set in the square perforations of the Ka-band patch, the size of E-band patch should be reduced as much as possible, otherwise, it will increase the difficulty of designing the Ka-band patch. Secondly, the spacing between antenna elements should be between 0.5 and 0.8 free space wavelengths to avoid far-out sidelobes. An antenna unit where four E-band parasitic patches and one Ka-band patch sharing the same aperture is shown in Figure 2. The size of the E-band parasitic patch is $E\_l \times E\_w$, and the E-band driven patch has the same size; the size of the Ka-band patch is $Ka\_l \times Ka\_w$; the distances between the horizontal adjacent and the vertical adjacent E-band patches are denoted as U_l and U_w respectively; the gaps between the E-band patch edge and the edge of perforated hole in the Ka-band patch are $d1$ and $d2$ in the horizontal and vertical directions respectively. It is clear that the horizontal length Ka_l of the Ka-band patch should larger than $U\_l + E\_l + 2d1$, and the vertical length Ka_w of the Ka-band patch should larger than $E\_w + U\_w + 2d2$. On the other hand, when used in
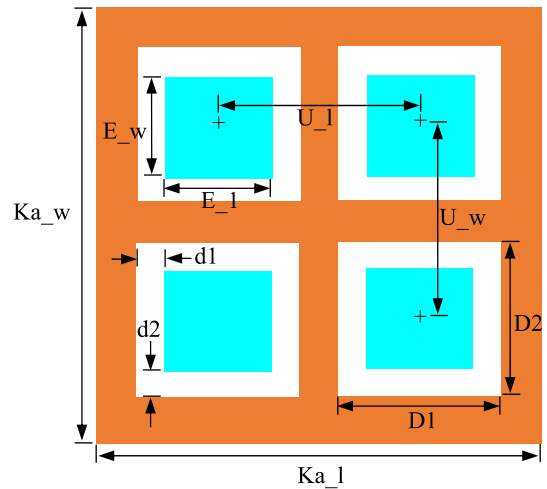

FIGURE 2. Four E-band patches and one Ka-band patch sharing the same aperture.
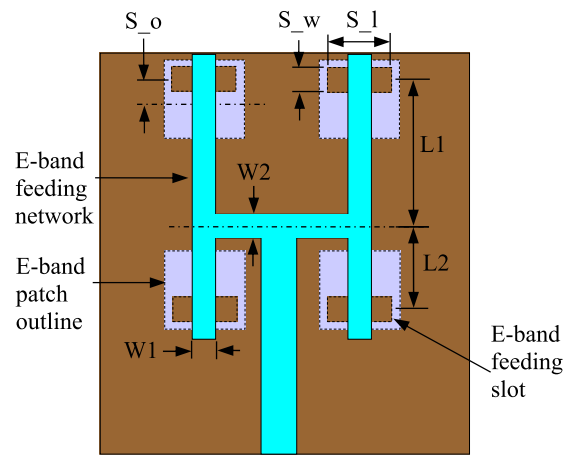

FIGURE 3. E-band feeding network.

the antenna array, the Ka-band patch size should not be too large to degrade the performance of the neighbouring E-band patches outside this Ka-band patch, so that Ka_l is set as: $Ka\_l \leq 2U\_l$ and Ka_w is set as: $Ka\_w \leq 2U\_w$.

The Ka-band patch is directly fed by microstrip line, however, the size of the Ka-band patch is restricted by the surrounding E-band patches, and it is difficult to design the input impedance of Ka-band patch exactly to 50ohm, so an impedance matching line (see figure 1) nearly 1/4 guided waves of the microstrip line is used to match the Ka-band patch to 50ohm microstrip line.

At higher frequency, it is difficult to feed the patches through probes or through direct connection of microstrip lines, so slot-coupling technique is used to feed the E-band patch, see Figure 3 which is the bottom view (refer to Figure 1) of PCB 3. The electromagnetic waves are transmitted by microstrip line at the bottom side of PCB 3 and then couple through the slots etched on the ground plane (top side of PCB 3) to the patch.

Through a lot of simulation and optimization, all parameters of the SAAU are determined, locked and listed in Table 1.
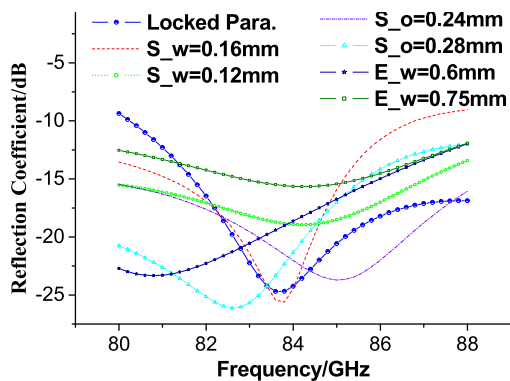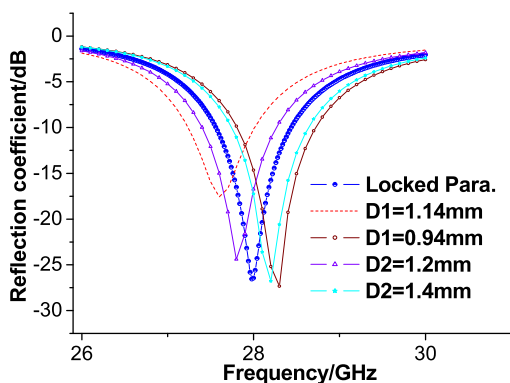
FIGURE 4. Simulated return loss of the SAAU. (a) E-band; (b) Ka-band.

TABLE 1. Shared aperture antenna parameters.

Parameter symbol	Parameter value (mm)	Parameter symbol	Parameter value(mm)
hPCB1	0.254	D1	1.3
hPCB2	0.254	D2	1.04
hPCB3	0.127	S_l	0.8
Ka_l	3.1	S_w	0.144
Ka_w	3.6	S_o	0.262
E_l	0.8	W1	0.25
E_w	0.7	W2	0.3
U_l	1.5	Ws	0.4
U_w	1.5		

The length of L1 plus L2 is about half the guided wavelength. The simulated reflection results of the antenna model of locked parameters are given in Figure 4, several other simulated results when changing only a single structure parameter in each simulating are added to Figure 4 for comparison. At E-band, as can be seen from Figure 4(a), parameter S_o mainly affects the center frequency of the antenna, parameter S_w mainly affects the reflection coefficient, while the parameter E_w affects not only the antenna center frequency but also the reflection coefficient. Usually, when it is necessary to change the size of the patch, which leads to poor reflection coefficient, one can always optimize S_o and S_w to restore good reflection characteristics. At Ka-band, the size of the perforated window mainly affects the center frequency (see Figure 4(b)), and the microstrip matching line (about a quarter wavelength) is used to ensure a good match.
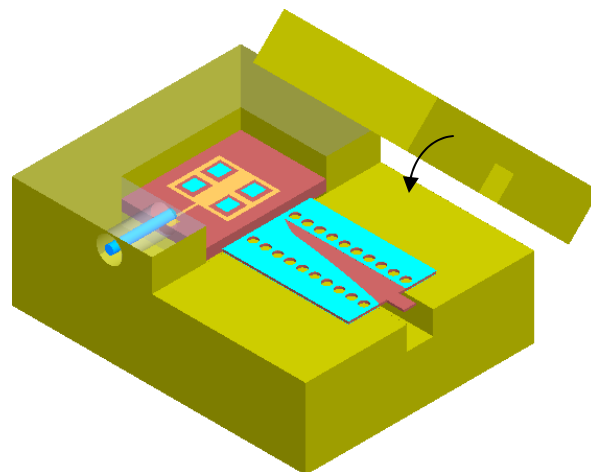

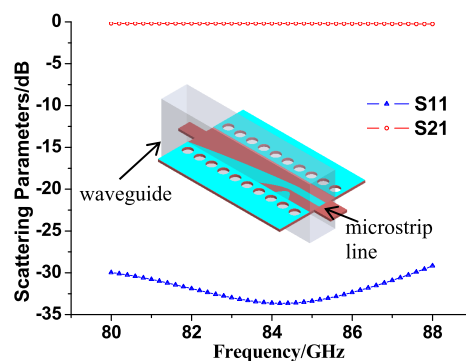**FIGURE 5.** A SAAU set in the metal cavity.

FIGURE 6. Antipodal fin-line waveguide to microstrip transition.

In order to verify the validness of our design, a prototype of the SAAU is fabricated for testing. The three laminated PCB layers of the unit are set in a metal cavity, the microstrip line of Ka-band port is connected to SMA connector by a through-wall manner, see Figure 5. However, at higher frequencies, directly connecting the microstrip line to SMA connector will result in large reflections, so the microstrip line of E-band port is converted to the standard waveguide port through an antipodal fin-line waveguide to microstrip transition [15], [16]. The antipodal fin-line waveguide to microstrip transition model and its simulated result is given in Figure 6.

The fabricated SAAU set in the metal cavity is shown in Figure 7. The measured reflection and radiation pattern are given and compared with the simulated results in Figure 8 and Figure 9 respectively. Due to the influence of the metal cavity, both the center frequencies of the two frequency bands have small deviations compared to the result of the no-metal-cavity model. The radiation patterns (Ka-band@28GHz and E-band@84GHz) of both bands are also affected by the metal cavity, for example there is a large discrepancy between the simulated and measured results of the H-plane radiation pattern in Figure 9(d), it is supposed to be due to the fact that at Ka-band the patch edges are closer to the wall of the metal cavity in H-plane than that in the E-plane. Similarly,
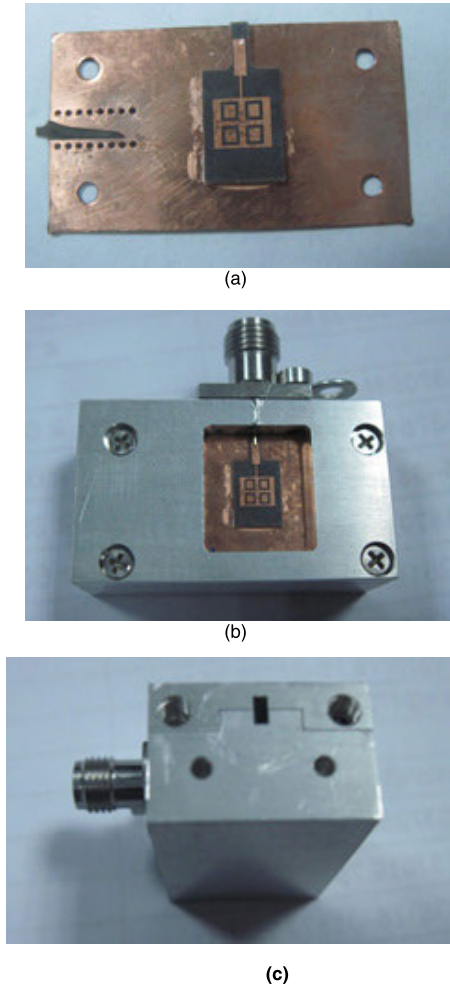
(a)

(b)

(c)

FIGURE 7. Fabricated SAAU. (a) PCB; (b) Top view of the SAAU set in the cavity; (c) Waveguide port view.

at E-band the simulated radiation pattern and the measured results of E-plane (Figure 9 (a)) agree worse with each other than that at H-plane (Figure 9(b)), because the E-plane of E-band coincides with the H-plane of Ka-band, and the patch edges are closer to the wall of the metal cavity in E-plane (of E-band) than that in the H-plane (of E-band).

III. DESIGN OF THE E/KA DUAL BAND SHARED APERTURE ANTENNA ARRAY

Based on the SAAU, an E/Ka dual-band shared aperture antenna array is constructed. The dual-band antenna array consists of a 2 × 4 Ka-band array and an 8 × 16 E-band array. In order to avoid grating lobe at larger angles at E-band, two additional E-band elements are inserted between two adjacent E/Ka SAAUs, and after a little adjust the patch element spacing for Ka-band and E-band are finally determined. The element spacing in the horizontal direction are $0.75\lambda_{Ka}$ (λ_{Ka} -wavelength of Ka-band center frequency) and $0.56\lambda_E$ (λ_E -wavelength of E-band center frequency) for Ka-band and E-band respectively, see Figure 10; the element spacing in the vertical direction are $0.56\lambda_{Ka}$ and $0.42\lambda_E$
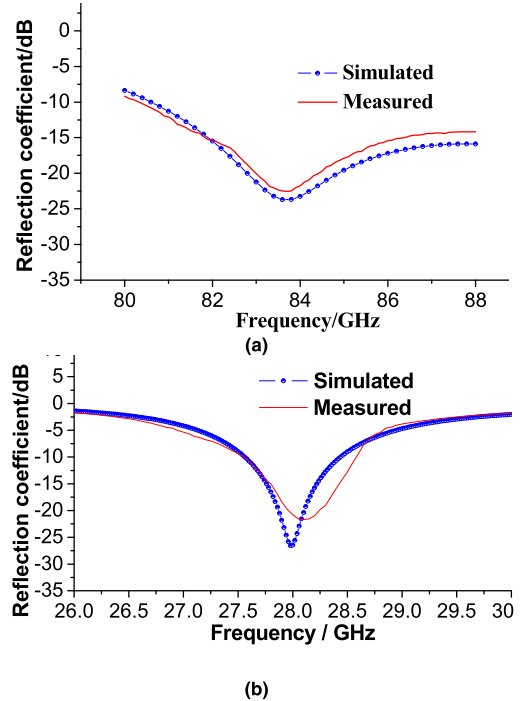

(a)

(b)

FIGURE 8. Return loss of the SAAU. (a) E-band; (b) Ku-band.

respectively. Due to the narrow space in the array, series-fed which is simple and more compact than parallel-fed is employed [12]. The series-fed network is shown in Figure 11, where port 1 ∼ n have the same port impedance Z_0 and are finally connected to the antenna units. RF power P incident at the sum port is distributed by the series-fed network to port 1 ∼ n, the distributed power obtained by port 1 ∼ N are $P_1, P_2, \ldots, P_n$ respectively, and $P_1 = P_2 = \ldots = P_n = P/n$. The inter-element line length between two adjacent ports is one guided wavelength (λ_g) for in-phase excitation. $Z_{in,1}, Z_{in,2} \ldots Z_{in,n-1}$ are the input impedance seen from port 1 ∼ n respectively and must satisfy equation (1)

$$Z_{in,1} = Z_0; Z_{in,2} = Z_0/2; \ldots Z_{in,n-1} = Z_0/(n-1); \quad (1)$$

The series-fed technique is applied in E-band feeding network as shown in Figure 12. E-band feeding network is more complicated than Ka-band network, for the input impedance of the E-band patch in the perforation of Ka patch is different from that out of the Ka patch. Thus, the impedance transformation is applied between two adjacent elements for obtaining equal amplitude power excitation. Parallel-fed is employed outside the array for reducing the design difficulty. In the design of Ka-band feeding network, cut-in slots at Ka-band element feed point is used to increase the impedance for better matching [13]. The Ka-band feeding network is shown in Figure 10, parallel-fed is also employed outside the array for reducing the design difficulty.
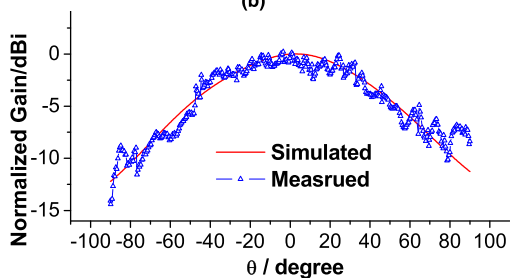
To verify the characteristics of the aperture-shared antenna array, a protype model (shown in Figure 13) is simulated using HFSS. The antenna array is also set in a cavity with a Ka-band SMA connector port and an E-band waveguide port.
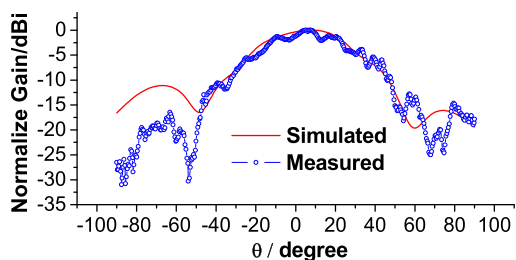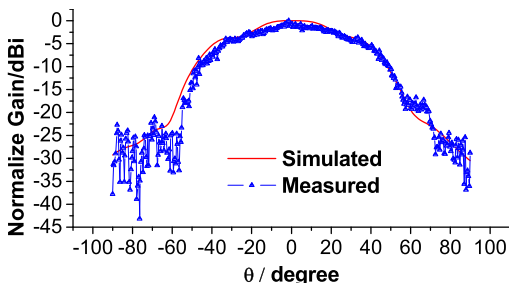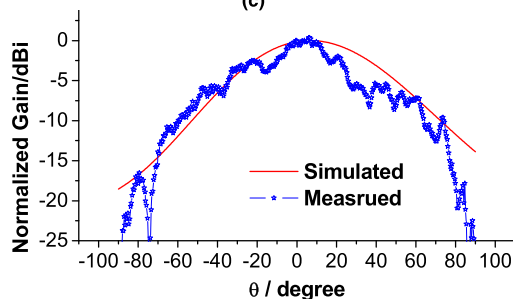
FIGURE 9. Radiation pattern of the SAAU. (a) E-plane of E-band; (b) H-plane of E-band;(c) E-plane of Ku-band; (d) H-plane of Ku-band.
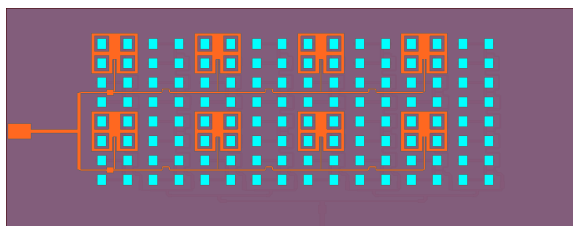

FIGURE 10. Top view of the shared aperture array and Ka-band feeding network.

The manufactured antenna array is shown in Figure 14. The measured results of the return loss and radiation pattern (Ka-band@28GHz and E-band@84GHz) are compared
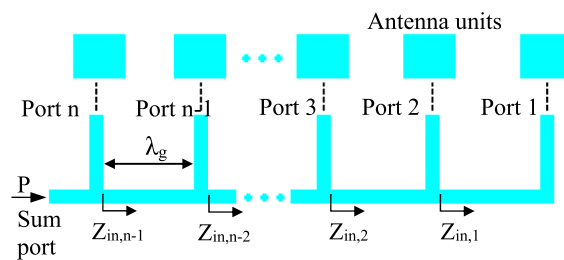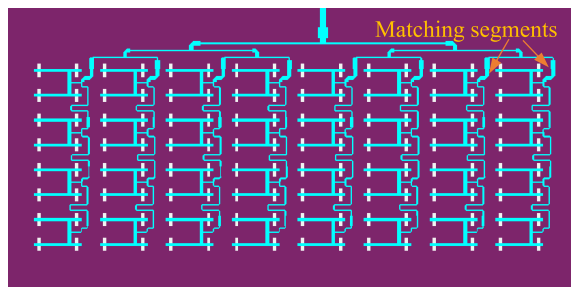

FIGURE 11. Series-fed network.

FIGURE 12. E-band feeding network.

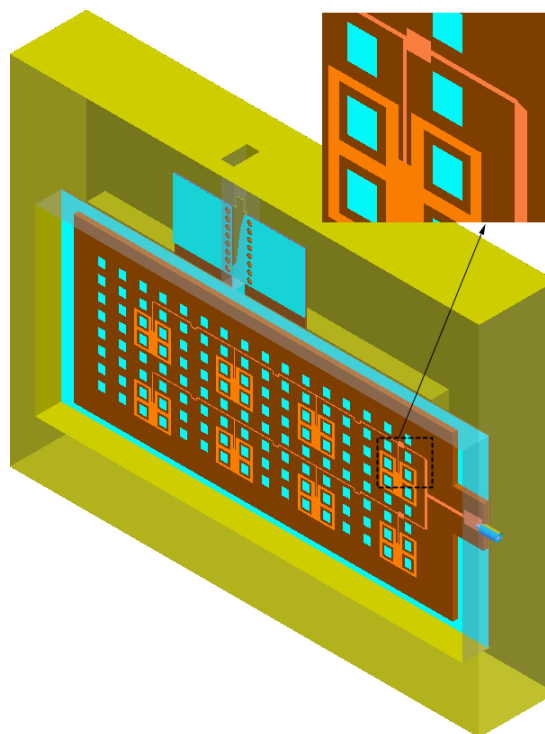**FIGURE 13.** Experimental model.

with the simulated ones and presented in Figure 15 and Figure 16 respectively.

It can be seen from Figure 15 and 16 that the antenna has 1GHz bandwidth (return loss < −10dB) for Ka-band and 3.6GHz (return loss < −10dB) for E-band; 15.5dB co-polarization gain for Ka-band and 24.7dB co-polarization gain for E-band; the cross-polarization level is lower than the

FIGURE 14. Fabricated shared aperture antenna array.
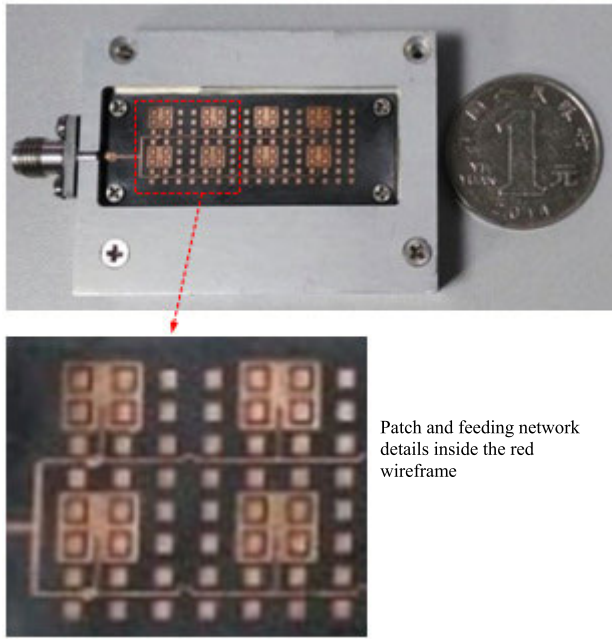
Patch and feeding network details inside the red wireframe
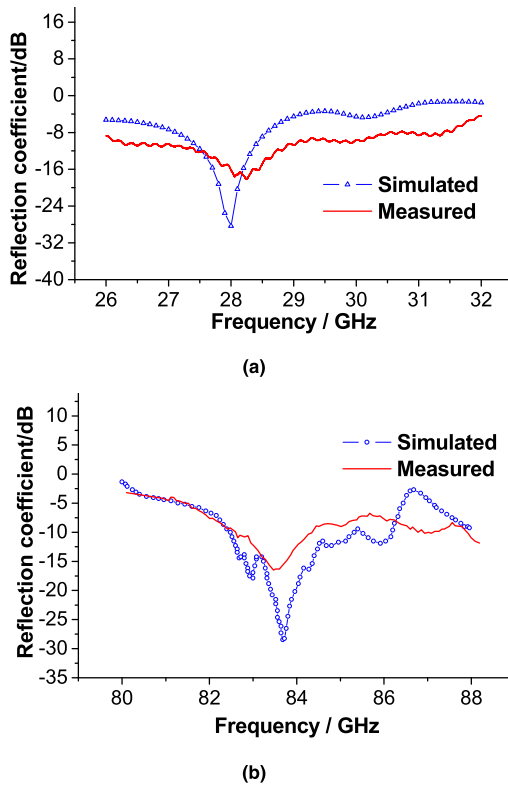
FIGURE 15. Return loss of the antenna array. (a) Ka-band; (b) E-band.

FIGURE 16. Radiation pattern of antenna array. (a) H-plane of E-band; (b) E-plane of E-band; (c) E-plane of Ka-band; (d) H-plane of Ka-band.

co-polarization level at the bore-sight direction in both planes by 33 dB at the E-band and 20 dB at the Ka-band. Generally, the gain of a single patch is 6 ∼ 7dBi, so theoretically, the gains of a 2 × 4 array and an 8 × 16 array can reach 15 ∼ 16dBi and 27 ∼ 28dBi respectively. The measured

gain of the Ka-band antenna is in good agreement with the theoretical value, while the measured gain of the E-band antenna is nearly 2.5dB lower than theoretical value, which is supposed to be due to two reasons: (1) the surface wave in

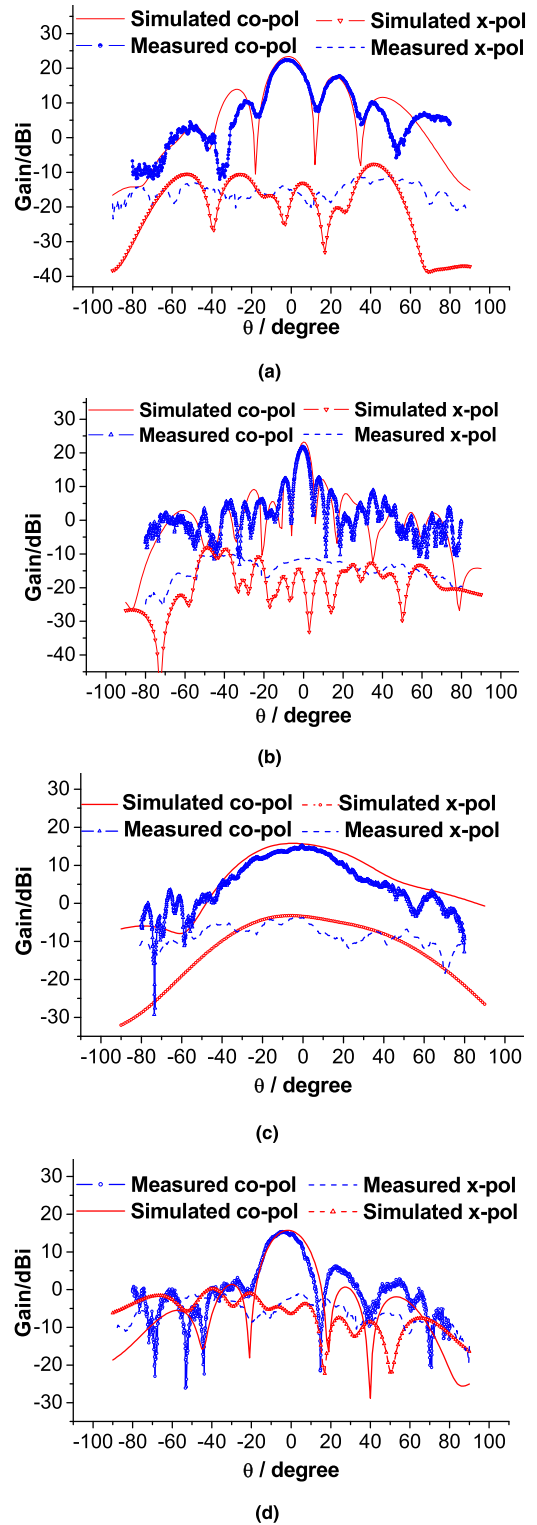PCB at E-band is more serious than that at Ka-band; (2) the patch spacing at E-band is smaller than that at Ka-band, so in E-band, there is relatively strong electromagnetic coupling between the patches which will disturb the phase consistency of the patches and eventually degrades the directivity of the antenna array. It must be pointed out that contrary to the case of the SAAU unit, the Ka-band patch array are closer to the metal wall of the cavity in E-plane than that in the H-plane, the E-band patch array are closer to the metal wall of the cavity in H-plane than that in the E-plane. Consequently, there is a larger discrepancy between the simulated and measured results of the radiation pattern in H-plane than in E-plane at E-band, while the opposite is true at Ka-band.

IV. CONCLUSION

This paper presented a design of E/Ka dual-band patch antenna array with shared aperture. The antenna array is designed of stack structure of three laminated PCBs. Ka-band and E-band patch radiators are all on the top surface of the stacked structure. A basic shared aperture unit consists of a Ka-band patch and four E-band patches; the Ka-band patch has four square perforations where four E-band patches are set. Two additional E-band elements are inserted between adjacent basic shared aperture units in order to avoid grating lobe at larger angles at E-band. The Ka-band patches in the array are fed directly with microstrip lines of the Ka-band feeding network. The E-band patches are coupling fed by the E-band power divider network through slots cut in the antenna ground, and E-band parasitic patches are added between the patch radiators and the coupling slots for bandwidth expansion. Series-fed technique combined with parallel-fed technique are used in the design of the Ka-band and the E-band feeding network as a compromise between the limited space and the design difficulty. It should be pointed out that in the design of shared aperture antenna array, the patch size is restricted, so the matching lines of feed network play a very important role in reducing the wave reflection. Finally, a dual-band shared aperture antenna array consists of a 2×4 Ka-band array and an 8×16 E-band array is designed. The shared aperture antenna array is simulated, fabricated and measured. In order to measure the E-band array, the main port of the E-band power divider is connected to a standard WR12 waveguide through an antipodal fin-line waveguide to microstrip transition. The measured return loss and radiation pattern are presented, and the measured results are consistent with the simulation results which shows the effectiveness of our design.

REFERENCES

[1] C. Salvador, L. Borselli, A. Falciani, and S. Maci, "A dual frequency planar antenna at S and X bands," *Electron. Lett.*, vol. 31, no. 20, pp. 1706–1707, Oct. 1995.
[2] T. A. Axness, R. V. Coffman, B. A. Kopp, and K. W. O'Hare, "Shared aperture technology development," *Johns Hopkins APL Tech. Dig.*, vol. 17, no. 3, pp. 285–294, Jul. 1996.
[3] S. Maci and G. B. Gentili, "Dual-frequency patch antennas," *IEEE Antennas Propag. Mag.*, vol. 39, no. 6, pp. 13–20, Dec. 1997.
[4] D. M. Pozar, D. H. Schaubert, S. D. Targonski, and M. Zawadski, "A dual-band dual-polarized array for spaceborne SAR," in *Proc. IEEE Int. Symp. Antennas Propaga.*, New York, NY, USA, Jul. 1998, pp. 2112–2115.
[5] L. L. Shafai, W. A. Chamma, M. Barakat, P. C. Strickland, and G. Seguin, "Dual-band dual-polarized perforated microstrip antennas for SAR applications," *IEEE Trans. Antennas Propag.*, vol. 48, no. 1, pp. 58–66, Jan. 2000.
[6] J. Granholm and N. Skou, "Dual-frequency, dual-polarization microstrip antenna development for high-resolution, airborne SAR," in *Proc. Asia–Pacific Microw. Conf.*, Dec. 2000, pp. 17–20.
[7] D. M. Pozar and S. D. Targonski, "A shared-aperture dual-band dual-polarized microstrip array," *IEEE Trans. Antennas Propag.*, vol. 49, no. 2, pp. 150–157, Feb. 2001.
[8] F. Qin, S. S. Gao, Q. Luo, C.-X. Mao, C. Gu, G. Wei, J. Xu, J. Li, C. Wu, K. Zheng, and S. Zheng, "A simple low-cost shared-aperture dual-band dual-polarized high-gain antenna for synthetic aperture radars," *IEEE Trans. Antennas Propag.*, vol. 64, no. 7, pp. 2914–2922, Jul. 2016.
[9] C.-X. Mao, S. Gao, Y. Wang, Q. Luo, and Q.-X. Chu, "A shared-aperture dual-band dual-polarized Filtering-Antenna-Array with improved frequency response," *IEEE Trans. Antennas Propag.*, vol. 65, no. 4, pp. 1836–1844, Apr. 2017.
[10] K. Li, T. Dong, and Z. Xia, "A broadband shared-aperture L/S/X-band dual-polarized antenna for SAR applications," *IEEE Access*, vol. 7, pp. 51417–51425, 2019.
[11] J. F. Zhang, Y. J. Cheng, Y. R. Ding, and C. X. Bai, "A dual-band shared-aperture antenna with large frequency ratio, high aperture reuse efficiency, and high channel isolation," *IEEE Trans. Antennas Propag.*, vol. 67, no. 2, pp. 853–860, Feb. 2019.
[12] E. A. Soliman, A. Vasylchenko, V. Volski, G. A. E. Vandenbosch, and W. De Raedt, "Series-fed microstrip antenna arrays operating at 26 GHz," in *Proc. IEEE Antennas Propag. Soc. Int. Symp.*, Jul. 2010, pp. 1–4.
[13] N. Boskovic, B. Jokanovic, M. Radovanovic, and N. S. Doncov, "Novel ku-band series-fed patch antenna array with enhanced impedance and radiation bandwidth," *IEEE Trans. Antennas Propag.*, vol. 66, no. 12, pp. 7041–7048, Dec. 2018.
[14] B.-L. Ooi, S. Qin, and M.-S. Leong, "Novel design of broad-band stacked patch antenna," *IEEE Trans. Antennas Propag.*, vol. 50, no. 10, pp. 1391–1395, Oct. 2002.
[15] E. G. Pnochak and N. A. Downey, "A new model for broad-band waveguide-to-microstrip transition design," *Microw. J.*, vol. 5, pp. 333–343, May 1988.
[16] M. J. Ahmed, "Impedance transformation equations for exponential, cosine-sqaared, and parabolic tapered transmission lines," *IEEE Trans. Microw. Theory Techn.*, vol. 29, no. 1, pp. 67–68, Jan. 1981.

ZONGXIN WANG was born in Yantai, Shandong, China, in 1970. He received the B.S. degree in microelectronics engineering from the University of Hunan, China, in 1993, the M.S. degree from the Institute of Mechanical Science, China, in 2001, and the Ph.D. degree from the School of Information Science and Engineering, Southeast University, China, in 2006.

He is currently an Associate Professor with the State Key Laboratory of Millimeter Waves, Southeast University. His research interests include PCB antenna array, slotted waveguide array, and antenna stealth technique.

ZEQIN HUANG was born in Fujian, China, in 1998. He received the B.S. degree in communication engineering from the Nanjing University of Technology and Science, Nanjing, China, in 2020. He is currently pursuing the M.S. degree in microwave engineering with Southeast University, Nanjing.

His current research interests include phased array antennas and ultra-broadband antennas.

● ● ●